ChemPubSoc Europe

DOI: 10.1002/ejic.201700983

EurJIC European Journal of Inorganic Chemistry

Full Paper

Photomagnetism

CLUSTER ISSUE

Direct Evidence of a Photoinduced Electron Transfer in Diluted "Molybdenum-Copper" Molecular Compounds

Nathalie Bridonneau,[a] Pierre Quatremare,[a] Hans Jurgen von Bardeleben,[b] Jean-Louis Cantin,[b] Sébastien Pillet,[c] El-Eulmi Bendeif,[c] and Valérie Marvaud*[a]

Dedicated to the memory of Professor Olivier Kahn

Abstract: For the first time, direct evidence of a photoinduced intramolecular electron transfer has been found in the "molybdenum-copper" family of cyanide complexes that corresponds to a $[Mo^{IV}–Cu^{II}]\rightarrow[Mo^{V}–Cu^{I}]$ transition. The design and synthesis of a diluted molecular system, $[Mo(Zn_{(1-x)}Cu_x)_2$-tren] (x = 0, ε, 1, 5 and 10 %, , with ε corresponding to ppm ratio), viewed as new model compounds, have allowed good characterization of the metastable states involved in the process and provided evidence for two different mechanisms. By using squid magnetometry, EPR spectroscopy and X-ray diffraction, the results of this study have confirmed not only the photoinduced electron transfer, but also supports the light-induced excited spin state trapping effect centred on the molybdenum, thought to be due to the presence of a high-spin state (S = 1). This article provides a better understanding of the photomagnetic behaviour in Mo-Cu complexes and reveals the importance of orbital overlap to differentiate the two effects.

Introduction

Molybdenum-copper complexes have attracted great attention over the past decade due to the interesting photomagnetic phenomena that have been reported for these systems.[1–10] Most of the compounds display a reversible photoinduced magnetic bistability that has been developed into various forms: three-dimensional networks,[11–13] molecular complexes,[14–18] high nuclearity clusters,[19,20] chains,[21,22] nanoparticles[23,24] and films.[25–27] In addition, the integration of Mo-Cu complexes viewed as magnetic switches into sophisticated architectures[28,29] has been performed with success as well as their transformation into promising materials with various properties.[30,31] However, a debate has emerged concerning the mechanism that might justify the related photomagnetic properties: loss of a ligand,[32] spin transition or electron transfer, the question remains open.[33–35] In this work we prepared reference compounds in an attempt to gain additional insight to support a better understanding of the photomagnetic behaviour. In particular, we suggest that two mechanisms may coexist, depending on geometric and orbital considerations.

For such a purpose, and as cleverly used for the study of light-induced bistability in iron(II) spin-crossover compounds,[36,37] we have designed diluted mixed crystals based on $Mo(Zn_{1-x}Cu_x)_2$ trinuclear complexes to clearly identify the metastable states of the photoinduced process. The highly diluted compounds are mainly associated with the $MoZn_2$ and MoCuZn species, whereas the concentrated samples are related to MoCuZn and $MoCu_2$ species.

We recently presented the new trinuclear compound $MoZn_2$-tren [tren = tris(2-aminoethyl)amine ligand], which exhibits clear evidence of a photoinduced spin transition involving the molybdenum centre: $Mo^{IV\text{-}LS}$ (S = 0)→$Mo^{IV\text{-}HS}$ (S = 1).[33] Following this result, and in an attempt to determine the photoinduced mechanism occurring in "molybdenum-copper" compounds, we doped the trimetallic $MoZn_2$ complex with various percentages of copper ions (ε, 1, 5 and 10, with ε corresponding to the ppm ratio). All the products, with different concentrations of Cu, were prepared for a specific purpose. Highly diluted copper compounds in a molybdenum-zinc matrix are of interest for analysing more specifically by EPR spectroscopy the heterotrimetallic complex MoCuZn. Thus, in this work we focused on the results obtained for the ε, 1 and 5 % Cu compounds, denoted respectively $Mo(Zn_{1-\varepsilon}Cu_\varepsilon)_2$-tren (**2**), $Mo(Zn_{0.99}Cu_{0.01})_2$-tren (**3**) and $Mo(Zn_{0.95}Cu_{0.05})_2$-tren (**4**), and their comparison with the previously described $MoZn_2$-tren complex (**1**), obtained with the purest Zn precursor. Highly concentrated compounds, such as **4** or $Mo(Zn_{0.9}Cu_{0.1})_2$-tren, (**5**; integrating MoCuZn and $MoCu_2$ complexes) are interesting in this regard for performing X-ray diffraction and magnetic studies using squid magnetometry.

[a] *IPCM-CNRS-UMR-8232, UPMC-Univ. Paris 6, cc 229, 4 place Jussieu, 75252 Paris Cedex 05, France*
E-mail: valerie.marvaud@upmc.fr
http://www.ipcm.fr/MARVAUD-Valerie
[b] *INSP-CNRS-UMR-7588, UPMC-Univ. Paris 6, 4 place Jussieu, 75252 Paris Cedex 05, France*
[c] *Université de Lorraine, CNRS, CRM2, Nancy, 54506 Vandroeuvre-les-Nancy, France*

Supporting information for this article is available on the WWW under https://doi.org/10.1002/ejic.201700983.

Results and Discussion

Crystallographic Studies

All the compounds were obtained by the slow addition of an aqueous solution of $K_4[Mo^{IV}(CN)_8]\cdot 4H_2O$ into a water/acetonitrile mixture of $Zn(OAc)_2$ and $Cu(OAc)_2$ with the tren ligand [or only $Zn(OAc)_2$ in the cases of **1** and **2** with different purity of the starting materials]. Large brown (**3–5**) or yellow (**1** and **2**) crystals (0.6 cm long) were obtained after 1–2 weeks of slow evaporation of the mother liquor. All the compounds of the family are isostructural. They crystallize in an orthorhombic system with the $Pca2_1$ space group; the cell parameters are a = 14.7778(3), b = 14.8566(3) and c = 31.0576(7) Å with a cell volume of V = 6818.6(2) Å^3 for the $MoZn_2$ complex (**1**) and a = 14.7573(5), b = 14.8266(4) and c = 30.9111(9) Å with a cell volume of V = 6763.3(3) Å^3 for the $Mo(Zn_{0.9}Cu_{0.1})_2$ compound (**5**). Two trimetallic molecules form the asymmetric unit. Each assembly is composed of one molybdenum centre linked to two zinc/copper complexes through cyanide bonds (Figure 1 and Table S1 in the Supporting Information). In such diluted $Mo(Zn_{1-x}Cu_x)_2$ systems, the zinc and copper atoms occupy the same site, so that the derived crystal structure (and the derived structural parameters, bond lengths, angles etc.) is an average of several possible molecular species (see Figure 1): $[MoZn_2]$, [MoZnCu] and $[MoCu_2]$, with $[MoZn_2]$ being the major one for high dilution values. Continuous shape measures showed that the two octacyanomolybdate complexes have a different coordination environment. One of them (Mo1) adopts a geometry close to a square-based antiprism, whereas the other one (Mo2) has a distorted environment that lies between a dodecahedron and square-based antiprism (see Table S2). The Mo–C and C≡N distances are similar for the two molybdenum centres, the six free cyanide ligands showing slightly longer distances than the bridging cyanides. The bridging cyanide angles are linear on the molybdenum side [174.4(5)–178.6(5)°], but very bent on the zinc/copper side. Four very different cyanide angles are thus reported, from 137.5(5)° for (Zn/Cu)4–N10≡C10 to 165.8(5)° for (Zn/Cu)3–C9≡N9. The four zinc/copper complexes adopt the same trigonal-bipyramidal geometry with similar Zn/Cu–N bond lengths. All the complexes are well isolated from each other, the shortest intermolecular metal–metal distance reported being 6.2341(8) Å.

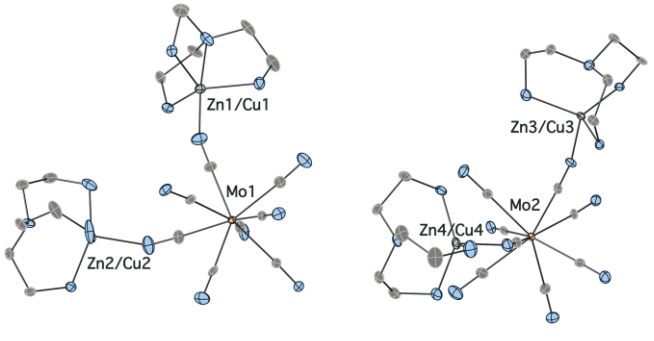

Figure 1. Crystallographic structure of the asymmetric unit of $Mo(Zn_{0.9}Cu_{0.1})_2$-tren, (**5**). Ellipsoids are drawn at the 30 % probability level.

Photomagnetic Studies

Photomagnetic measurements were realized on both crystalline samples and homogeneous powders obtained from ground crystals. All experiments performed on compounds **4** and **5** showed a photomagnetic response. The effect was more pronounced for diluted compound **4** (5 %) due to a higher photoconversion efficiency. For this reason, we report in detail on the photomagnetic studies of **4** (5 %), the other being consistent with our interpretation (see the Supporting Information). Before irradiation, compound **4** exhibits paramagnetic behaviour originating from the independent Cu^{II} centres ($3d^9$, S = 1/2), the Mo^{IV} ions being diamagnetic ($4d^2$, S = 0). The magnetization versus field curve was satisfactorily simulated by using Brillouin's function for an S = 1/2 spin (g = 2.1) corresponding to the expected percentage of copper ions (i.e., 5.92 % of Cu^{II} for **4**, in accordance with the compound's elemental analysis, which showed 5.62 % of copper). The sample was then irradiated under an applied field of 1 kOe using blue light (λ = 405 nm). An immediate increase in the recorded magnetization was observed and saturation occurred typically after 8 hours (see Figure S4 in the Supporting Information). After switching off the laser, the sample was cooled to 2 K and then the magnetization data were recorded in heating mode (2–300 K).

The magnetic susceptibility data recorded after irradiation showed a clear increase, as depicted in Figure 2. A maximum of the $\chi_m T$ product is observed at 20 K with a value of 0.61 cm^3 K mol^{-1} (Figure 2b). Heating the compound to room temperature caused a gradual decay of the process with complete relaxation observed at around 200 K.

Comparing this photoinduced $\chi_m T$ curve with that obtained for the $MoZn_2$-tren compound (**1**) is very informative (Figure 3). Indeed, both curves show differences even at very low temperature, the maximum $\chi_m T$ values being reached at different temperatures (20 K for **4**, 8.5 K for **1**). The relaxation temperature of **4** is significantly different to that of the pure zinc compound: 200 K for **4** and around 90 K for **1**. All these data suggest that even though **4** contains only 5 % of Cu^{II} ions, their presence plays an important role in the photoinduced mechanism, which is visible over a large temperature range.

The magnetization curve recorded for **4** also shows an important increase after irradiation (Figure 2a), with an observed evolution from 0.12 μ_B to 0.70 μ_B and no clear saturation at 50 kOe. Because of the incorporation of Cu^{II} ions into the structure, simulation of this photoinduced magnetization curve is not an easy task. Indeed, different potentially photoactive species must be considered, namely $[MoZn_2]$, [MoZnCu] and $[MoCu_2]$, all of them associated with different spin values depending on the hypothesis considered: spin transition or photoinduced electron transfer (Table 1). Also, magnetic experiments performed on **1** suggest that the different coordination environment of the two molybdenum centres causes an unequal response to light irradiation, because in all our attempts it was never possible to achieve more than around 50 % photoconversion of the compound.[33] It was suggested that the specific geometry of the coordination polyhedron as a distorted antiprism might justify the stabilization of the triplet state.

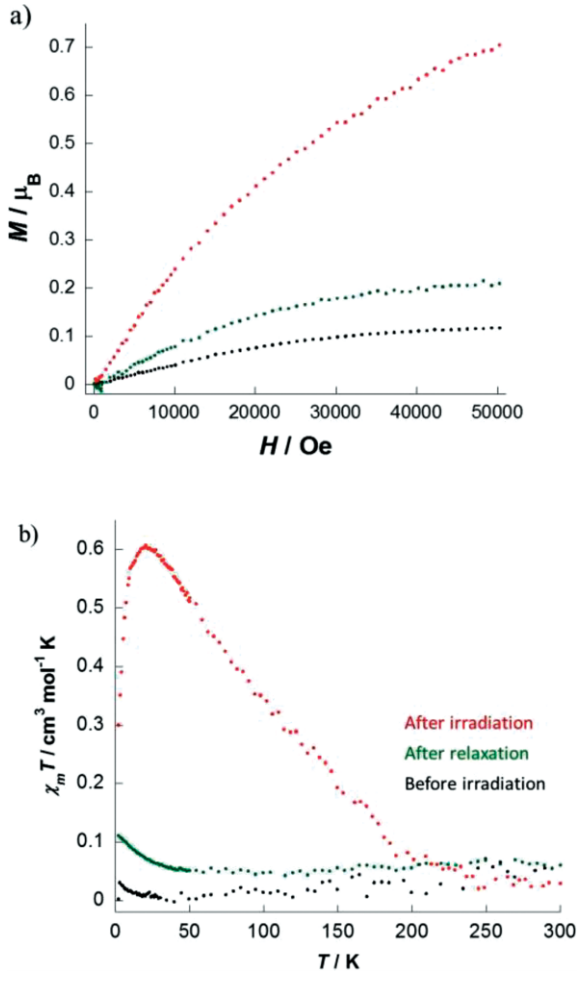

Figure 2. a) Evolution of the magnetization vs. field at 2 K upon light irradiation of compound **4** and b) evolution of the thermal susceptibility vs. temperature, upon light irradiation of compound **4**.

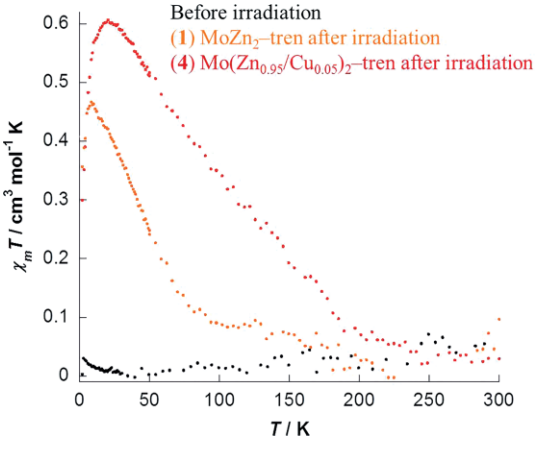

Figure 3. Comparison of the evolution of the thermal susceptibility vs. temperature upon light irradiation of compounds **1** and **4**.

The present study clearly evidences that the increase in the overall magnetization confirms the presence of high-spin molybdenum, even in the presence of copper cations (whereas, considering only the hypothesis of electron transfer, a decrease in the magnetization compared with pure $MoZn_2$ would have been detected, the spin being only delocalized from the Cu to the Mo). It appears as well that the MoCuZn photoactive species might be induced for more than 50 % of the compound, which indicates that the photomagnetic process, in the presence of copper ions, is apparently systematically effective.

Table 1. Metastable states accessible for the $[Mo(Zn_{(1-x)}Cu_x)_2$-tren] compounds and their corresponding spin values.

Species	Metastable states	Spin
$MoZn_2$[a]	$[Mo^{IV\text{-}HS}Zn_2]$	1
MoCuZn	$[Mo^{IV\text{-}HS}ZnCu^{II}]$	3/2
	$[Mo^{V}ZnCu^{I}]$	1/2
$MoCu_2$	$[Mo^{IV\text{-}HS}Cu^{II}_2]$	2
	$[Mo^{V}Cu^{I}Cu^{II}]$	1

[a] See ref.[33]

Upon increasing the copper ratio, the photomagnetic effect disappears. The compounds are still photoactive but the overall magnetization decreases regularly, which suggests that a different mechanism occurs, probably due to photoinduced electron transfer from Mo^{IV} to Cu^{II} leading to Mo^{V} and Cu^{I}.

Photocrystallography

To confirm this assumption, single-crystal XRD experiments were carried out under irradiation for compound **5**. Photocrystallography is the method of choice to describe the modification of structures and charge densities in photoactive compounds. By using this technique, informative data can be obtained, especially when comparing the low-spin state to the metastable high-spin state during LIESST (light-induced excited spin state trapping) phenomena.[38]

Contrary to what was observed for the $MoZn_2$ complex (**1**),[33] no amorphization of the doped MoZnCu samples **4** and **5** was observed during the XRD experiments performed under light irradiation. Photodifference maps were calculated to analyse the light-induced changes in electron density and to identify the related structural changes upon transition from the ground state to the excited state (see Figure S2 in the Supporting Information). The main difficulty is to differentiate the effect induced by the high-spin molybdenum that is expected for the major product, $MoZn_2$, to other possible mechanisms. Full crystallographic measurements and refinement details are given in the Supporting Information.

The photodifference map calculated for sample **5** is very similar to that already reported for sample **1**.[33] It shows, in particular, that only the Mo2–C10–N10–Zn4/Cu4 fragment is strongly modified by photoirradiation at 405 nm, in addition to an increase in the Mo2–Zn4/Cu4 distance. We consider that these two characteristics are the structural signature of the photoexcited state of $[MoZn_2]$ species owing to the photoinduced spin transition $Mo^{IV\text{-}LS}$ ($S = 0$)→$Mo^{IV\text{-}HS}$ ($S = 1$). This is in agreement with the photomagnetic results discussed above.

The average refined structure of the photoirradiated state provides additional qualitative information. The corresponding ORTEP plots (see Figure S3 in the Supporting Information) show that the Mo1 molecule is not strongly affected by photoirradia-

tion, in agreement with the photodifference maps. In contrast, the Mo2–C10–N10–Zn4/Cu4 fragment shows exaggeratedly enlarged atomic ellipsoids, corresponding to a superposition of several structural conformations different from the ground state (compare Figure S3 top and bottom). In particular, the cyanide C10–N10 ligand undergoes a strong displacement in the photoirradiated state, inducing in turn a drastic decrease (increased bending) of the cyanide bond angle C10–N10–Zn4/Cu4, which favours the trapping of Cu^{I}, as discussed below. This effect was not observed for **1**; it is therefore the structural signature of an additional photoexcitation process. Photoinduced linkage isomerism of the C10–N10 cyano group could explain the photocrystallographic evidence, as already observed by Coppens and co-workers in nitroprusside[39] or in iron hexacyanochromate compounds.[40] However, from the present results, and taking into account the reversibility of the process, we do not have any evidence to confirm such a hypothesis.

Figure 4 shows the superposition of the two observed structures before and after irradiation of the compound. Only one of the two molecules is presented here, the other one exhibiting absolutely no structural differences before and after irradiation. In contrast, the structure depicted below exhibits structural modifications, observed here for the first time, concerning the atomic positions of Mo2 and (Zn/Cu)4, the tren ligand as well as the cyanide bond angle C–N–(Zn/Cu). It is worth noting that these modifications are located around the Zn/Cu centre connected to the molybdenum through the most bent cyanide angle [137.5(5)°].

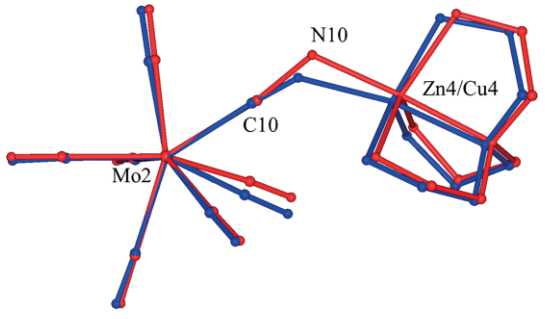

Figure 4. Superposition of the diffraction structures obtained before (blue) and after (red) light irradiation.

For the first time, structural modifications of the tren ligand are also observed that are in good agreement with possible structural change that might be induced by a change in the oxidation state of copper. These structural modifications strongly suggest the possibility of an electronic pathway through the cyanide bond, as well as a preferential crystallographic position to trap the Cu^{I} species. This result is consistent with a photoinduced electron transfer that may occur when copper ions occupy selectively the Zn4/Cu4 position. This might explain why the effect occurs as a function of the copper ratio, that is, in highly concentrated species.

EPR Spectroscopy

From the magnetization measurements of the highly diluted compounds, we have concluded that the photoinduced fraction is mainly due to high-spin molybdenum-based complexes. From photocrystallography, it seems that photoinduced electron transfer can occur for a copper ion in a specific location. EPR spectroscopy, a powerful and highly sensitive technique, has been applied to gain a better insight into the photoinduced mechanism.

EPR experiments were carried out on polycrystalline samples of **2**–**4** at T = 4 K using the same conditions of light irradiation as were used for the magnetization measurements. Before irradiation, all compounds showed EPR spectra of Cu^{II} with either resolved or unresolved hyperfine interactions characterized by a g value of g_{iso} = 2.13. Compounds **3** and **4** showed EPR spectra of Cu^{II} with a resolved hyperfine interaction between the electronic spin (S = 1/2) and the nuclear spin (^{63}Cu, I = 3/2, 69.17 % abundance and ^{65}Cu, I = 3/2, 30.83 % abundance). Low-temperature photoexcitation of compounds **2** and **3** produced an immediate change in the EPR spectra. First, new spectra are observed in the half-field region (1200–2200 G) attributed to weakly allowed Δm_s = 2 transitions of the Mo^{4+} centre with a spin S = 1 ground state. As both **2** and **3** are predominantly composed of [$MoZn_2$-tren] molecular entities, these spectra were expected. In parallel, the initial Cu^{II} spectra are quenched and different spectra are observed at higher fields characterized by the line shape of a powder spectrum with weak g-factor anisotropy that can be simulated with g values of $g\perp$ = 1.992 and $g\parallel$ = 1.960. These spectra have been previously reported in the literature[41,42] and attributed to Mo^{V} with a hyperfine (HF) interaction with the two isotopes ^{95}Mo (I = 5/2, 15.72 %) and ^{97}Mo (I = 5/2, 9.46 %). Figure 5 shows the evolution of the EPR spectra of **2** before and after light irradiation. After approximately 10 minutes of light irradiation the intensity of the EPR spectrum is saturated. Switching the light off produced no evolution of the photoinduced signal. Heating the compound to room temperature led to a gradual disappearance of the Mo^{V} and $Mo^{IV\text{-}HS}$ signals, which clearly indicates the reversibility of the process.

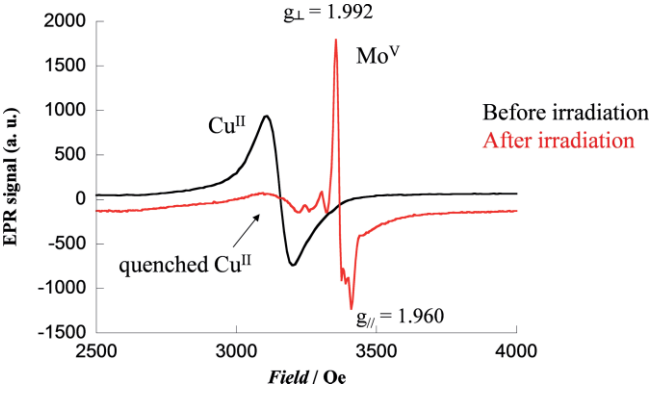

Figure 5. Evolution of the EPR spectra before (black) and after (red) irradiation of compound **2**.

In the case of compound **3**, which contains a higher ratio of copper ions (1 %), the Mo^{V} spectrum is still visible, but an additional spectrum is observed at g = 4 showing a resolved HF interaction with one Cu nucleus, which gives rise to the charac-

teristic quadruplet structure. This spectrum has been attributed to a high-spin $S = 3/2$ $Mo^{IV\text{-}HS}$–Cu^{II} complex with large zero-field splitting parameters (Figure 6).

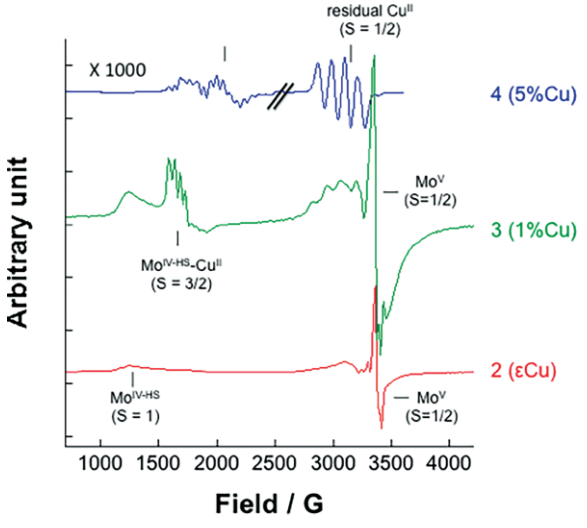

Figure 6. EPR spectra of compounds **2** (red), **3** (green), and **4** (blue) after irradiation.

In compound **4**, the residual Cu^{II} signal was too strong to allow the detection of the Mo^{V} spectrum. After photoexcitation we observed once again the high-spin $S = 3/2$ $Mo^{IV\text{-}HS}$–Cu^{II} ($S = 3/2$) spectrum, but with a modified g factor (Figure 6). This high-spin spectrum is weak compared with that attributed to residual Cu^{II} ($S = 1/2$) and disappears when the copper ratio is further increased. This might be explained by 1) the formation of Mo complexes with more than one Cu ion modifying the photoexcitation processes and 2) the thermal instability of the photoconversion.

To validate these attributions, we simulated the spectra of the Mo^{V} ($S = 1/2$) and $Mo^{IV\text{-}HS}$–Cu^{II} ($S = 3/2$) species by using the Bruker Simfonia program; the results gave good agreement with the experimental findings. Figure 7 and Figures S9–S11 in the Supporting Information show the experimental and simulated EPR powder spectra.

Although the fits are satisfactory, they might be still further improved by the use of fully powdered samples. In our case we used polycrystals for better optical excitation efficiency and phase purity (see the Supporting Information for details).

Nevertheless, the magnetization measurements confirmed that the main oxidation state of Mo in the highly diluted compounds is $Mo^{IV\text{-}HS}$ ($S = 1$). In the presence of copper atoms in close proximity, this high-spin species leads to a ferromagnetic exchange interaction and the formation of the high-spin $S = 3/2$ complex. As the copper ratio increases, photoinduced electron transfer operates, which is increasingly effective. The EPR signal of Mo^{V}–$Cu^{I}Cu^{II}$ species with $S = 1$, which might have been expected for higher Cu ratios, is not observed or partly masked by the copper signal of unreactive species. Nevertheless, in the diluted mixed crystals based on $Mo(Zn_{1-x}Cu_x)_2$ trinuclear complexes, the EPR spectra unambiguously show the presence of two mechanisms: Spin transition centred on the molybdenum and photoinduced electron transfer.

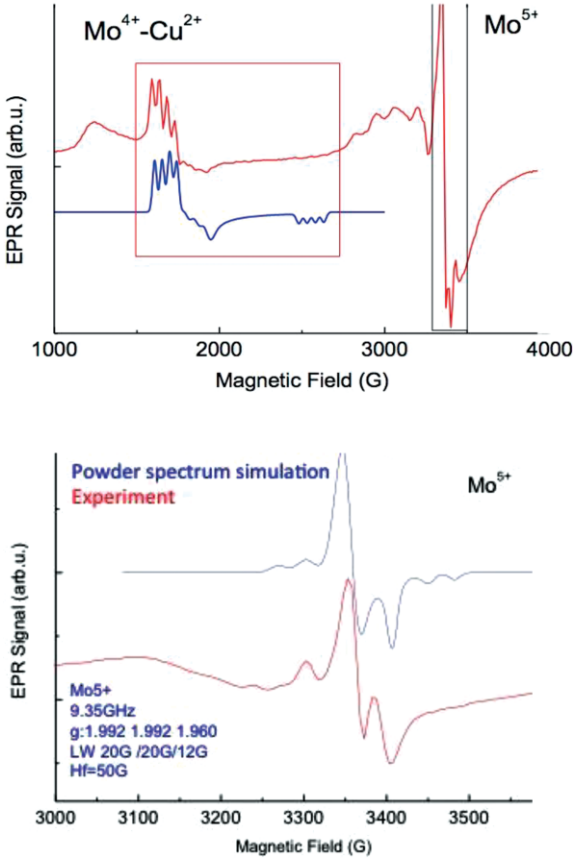

Figure 7. Theoretical and experimental EPR spectra of $Mo^{IV\text{-}HS}$–Cu^{II} ($S = 3/2$, upper) and Mo^{V} ($S = 1/2$, lower).

Discussion

Taking into account all these results, we can suggest the following interpretation of the photomagnetic behaviour in the $Mo(Zn_{1-x}Cu_x)_2$-tren complex and more generally in copper octacyanometallate compounds.

The photoinduced spin transition that has been evidenced in a molybdenum-zinc complex[33] has been confirmed, yielding a LIESST effect on the molybdenum, a 4d transition-metal ion. But it appears that the presence of copper in the proximity of molybdenum might stabilize the metastable state by partial electron delocalization, as already evoked in the literature.[43–45] This is valid for copper atoms that present orbital overlap, as observed in the present case when the cyanide ligand is linear and is revealed by a higher relaxation temperature. But in the specific case of a bent cyanide, we can suppose that the electron can be transferred and localized on the copper atoms and trapped in the charge-separated state, Mo^{V}–$Cu^{I}Cu^{II}$, in good agreement with the photoinduced electron-transfer hypothesis.

This might explain why the two mechanisms occur and indicates the importance of orbital overlap in the stabilization of the metastable states.

Olivier Kahn developed a model combining two magnetic orbitals with different symmetries that allows the magnetic properties to be predicted: strict orthogonality favours ferromagnetic exchange whereas interaction between overlapping

orbitals results in antiferromagnetism.[46] This simple orbital model of the magnetic interaction phenomenon works well and has been illustrated by many examples. Therefore, among others, we have described the manner in which the magnetic exchange interaction is mediated by the cyanide ligand and is therefore affected by the bridging angles.[47] In nickel hexacyanochromate complexes, for instance, the angle controls the overlap between the two magnetic orbitals centred on the two metallic ions and the delocalization of the spin density on the nitrogen atom.[48] Similarly, it appears that in the case of copper octacyanometallate compounds, in the presence of a linear ligand that allows electron delocalization, the high-spin state is favoured. However, as soon as the bridging angle is bent, the orbital overlap decreases, supporting the trapping of Cu^{I} and the charge-separated state, $Mo^{V}Cu^{I}$. Figure 8 and Figure 9 illustrate such an interpretation focusing on the significance of cyanide bending and orbital considerations. This is valid for a tren ligand associated with a trigonal-bipyramidal geometry around the copper ion, but this might be transposed to other geometries. DFT calculations are in progress to validate such a hypothesis and will be fully published elsewhere.

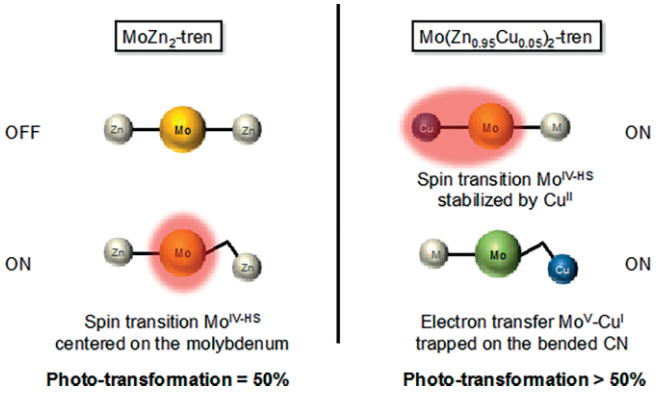

Figure 8. Scheme illustrating the two mechanisms: the spin transition centred on molybdenum (left) or the spin transition on molybdenum stabilized by electron delocalization, observed for linear cyanide compounds, or photoinduced electron transfer valid for distorted cyanide ligands (right).

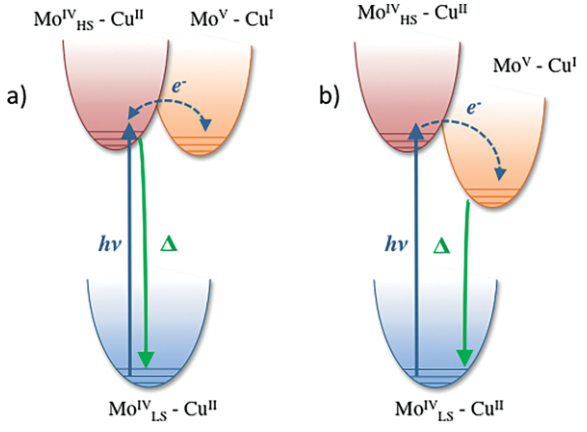

Figure 9. Potential energy curves illustrating the two mechanisms: spin transition on molybdenum (left) or photoinduced electron transfer (right).

To illustrate the two mechanisms, the potential energy curves might be helpful (Figure 9). In the case of the spin transition on molybdenum stabilized by electron delocalization, we may consider that the two excited levels $Mo^{IV\text{-}HS}$–Cu^{II} and $Mo^{V\text{-}HS}$–Cu^{I} are close in energy. The overlapping of the orbitals enhances the stability of the metastable state $Mo^{IV\text{-}HS}$–Cu^{II} ($S = 3/2$).

Concerning the photoinduced electron transfer that is observed for distorted cyanide ligands, the metastable state is trapped and then dissociates by electron transfer to yield the Mo^{V}–Cu^{I} species ($S = 1/2$).

Conclusion

We have synthesized the model trimetallic compounds $Mo[Zn_{(1-x)}Cu_x]_2$-tren, which have enabled us to unambiguously demonstrate the existence of high-spin molybdenum as well as photoinduced electron transfer from molybdenum to copper through a cyanide bridge $Mo^{IV}Cu^{II} \rightarrow Mo^{V}Cu^{I}$.

We have previously demonstrated the importance of the particular geometry of the octacyanometallate moiety to stabilize the high-spin state of the molybdenum: the specific geometry of the coordination polyhedron (distorted antiprism) justifies the stabilization of the triplet state.[33] In this paper we have also demonstrated the importance of the orbital overlap of the cyanide linkage in the stabilization of the metastable states. Thus, we have shown that two effects are present and that the two possible mechanisms co-exist: without copper only the spin transition centred on the molybdenum is observed, whereas in the presence of copper, depending on the bridging angle, we may observe a spin transition stabilized by Cu^{II} or electron transfer corresponding to the Mo^{IV}–$Cu^{II} \rightarrow Mo^{V}Cu^{I}$ transition. This provides a better understanding of the photomagnetic properties of cyanide-bridged molybdenum-copper complexes, which are more complicated than they appear at first glance.

Experimental Section

Materials and Methods: IR spectra were recorded as KBr disks with a Bio-Rad Win-IR FTS 165 spectrometer (250–4000 cm^{-1}, 4 cm^{-1} resolution).

Crystallographic data were collected with a Microfocus Supernova diffractometer. Unit-cell parameter refinement, integration and data reduction were carried out by using the Crysalis program (Oxford Diffraction). Crysalis was also used for scaling and analytical absorption corrections. In the WinGX suite of programs, the structure was solved with SHELXL-2014 and refined by full-matrix least-squares methods also with SHELXL-2014. Simfonia is a simulation program for EPR powder spectra edited by Bruker (more information may be obtained on acif.ucr.edu).

CCDC 1568691 (for **5**) contains the supplementary crystallographic data for this paper. These data can be obtained free of charge from The Cambridge Crystallographic Data Centre.

Synthesis: Caution! Cyanides are very toxic and must be handled with care.

Compounds **3**–**5** were prepared by the following general methods.

$Mo(Zn_{0.95}Cu_{0.05})_2$-tren, $[Mo(CN)_6\{(\mu CN)Zn_{0.95}Cu_{0.05}C_6H_{18}N_4\}_2]\cdot(H_2O)_{10}$ (4): The tren ligand [tris(2-aminoethyl)amine, 83 mg, 0.56 mmol, 4 equiv.] was dissolved in water/acetonitrile (1:1, v/v, 10 mL) and added to a mixture of $[Zn(OAc)_2]\cdot 2H_2O$ (117 mg, 0.54 mmol, 3.8 equiv.) and $[Cu(OAc)_2]\cdot 2H_2O$ (5.6 mg, 0.028 mmol, 0.2 equiv.) dissolved in the same solvent. After stirring for a few minutes, a solution of $K_4[Mo^{IV}(CN)_8]\cdot 2H_2O$ (70 mg, 0.14 mmol, 1 equiv.) was added dropwise without agitation. After filtration the solution was left to slowly evaporate in the dark, giving brown crystals within a week. Yield: 75 %. IR (KBr): $\tilde{\nu}$ = 3200, 2950, 2147, 2121, 2107, 2098, 1602, 1456 cm^{-1}. $C_{20}H_{56}Cu_{0.1}MoN_{16}O_{20}Zn_{1.9}$ (1067.27): calcd. C 30.39, H 28.35, Cu 0.89, Mo 12.14, N 5.48, Zn 16.55; found C 30.35, H 28.36, Cu 0.89, Mo 12.31, N 5.22, Zn 16.31; the elemental analysis revealed a presence of 5.62 % of copper in the material.

Compounds **1** and **2** were synthesized similarly by using zinc acetate of different quality: the highest purity precursor for **1** and per analysis purity for **2**.

$MoZn_2$-tren, $[Mo(CN)_6\{(\mu\text{-}CN)ZnC_6H_{18}N_4\}_2]\cdot(H_2O)_{10}$ (1): The tren ligand [tris(2-aminoethyl)amine, 83 mg, 0.56 mmol, 4 equiv.) dissolved in water/acetonitrile (1:1, 10 mL) were added to a solution of $[Zn(OAc)_2]\cdot 2H_2O$ (purity 99.999 %, 124 mg, 0.56 mmol, 4 equiv.) in the same solvent mixture. The solution was stirred for a few minutes before adding carefully (dropwise) a solution of $K_4[Mo^{IV}(CN)_8]\cdot 2H_2O$ (70 mg, 0.14 mmol, 1 equiv.) without agitation. The solution was filtered and then left to slowly evaporate in the dark. Yellow crystals were obtained within a week. Yield: 80 %. IR (KBr): $\tilde{\nu}$ = 3200, 2950, 2147, 2121, 2107, 2098, 1602, 1456 cm^{-1}. $C_{20}H_{56}MoN_{16}O_{20}Zn_2$ (1067.48): calcd. C 30.39, H 28.35, Mo 12.14, N 5.48, Zn 16.55; found C 30.49, H 28.09, Mo 12.15, N 5.28, Zn 16.94.

Acknowledgments

This research has been supported by the Centre National de la Recherche Scientifique (CNRS)-UMR-8232, UPMC, the Université de Lorraine, the French Ministry of Research, ANR Switch (2010-Blan-712) and ANR E-storic (14-CE05-0002). The authors thank Sébastien Blanchard for fruitful discussions.

Keywords: Photomagnetism · Electron transfer · Spin transition · Copper · Molybdenum · Magentic properties

[1] A. Bleuzen, V. Marvaud, C. Mathonière, B. Sieklucka, M. Verdaguer, *Inorg. Chem.* **2009**, *48*, 3453.
[2] O. Sato, J. Tao, Y.-Z. Zhang, *Angew. Chem. Int. Ed.* **2007**, *46*, 2152; *Angew. Chem.* **2007**, *119*, 2200.
[3] D. Aguila, Y. Prado, E. S. Koumousi, C. Mathonière, R. Clerac, *Chem. Soc. Rev.* **2016**, *45*, 203.
[4] A. Bousseksou, G. Molnar, L. Salmon, W. Nicolazzi, *Chem. Soc. Rev.* **2011**, *40*, 3313.
[5] M. A. Halcrow, *Coord. Chem. Rev.* **2009**, *253*, 2493.
[6] S. Hayami, Y. Komatsu, T. Shimizu, H. Kamihata, Y. N. Lee, *Coord. Chem. Rev.* **2011**, *255*, 1981.
[7] J. Olguin, S. Brooker, *Coord. Chem. Rev.* **2011**, *255*, 203.
[8] O. Sato, *Nat. Chem.* **2016**, *8*, 644.
[9] X.-Y. Wang, C. Avendano, K. R. Dunbar, *Chem. Soc. Rev.* **2011**, *40*, 3213.
[10] D. Unruh, P. Homenya, M. Kumar, R. Sindelar, Y. Garcia, F. Renz, *Dalton Trans.* **2016**, *45*, 14008.
[11] T. Hozumi, K. Hashimoto, S.-i. Ohkoshi, *J. Am. Chem. Soc.* **2005**, *127*, 3864.
[12] G. Rombaut, M. Verelst, S. Golhen, L. Ouahab, C. Mathonière, O. Kahn, *Inorg. Chem.* **2001**, *40*, 1151.
[13] Y. Umeta, S. Chorazy, K. Nakabayashi, S.-i. Ohkoshi, *Eur. J. Inorg. Chem.* **2015**, 1980.
[14] H. T. Xu, O. Sato, Z. H. Li, J. P. Ma, *Inorg. Chem. Commun.* **2012**, *15*, 311.
[15] C. Mathonière, R. Podgajny, P. Guionneau, C. Labrugere, B. Sieklucka, *Chem. Mater.* **2005**, *17*, 442.
[16] S.-i. Ohkoshi, N. Machida, Z. J. Zhong, K. Hashimoto, *Synth. Met.* **2001**, *122*, 523.
[17] O. Stefanczyk, A. M. Majcher, M. Rams, W. Nitek, C. Mathonière, B. Sieklucka, *J. Mater. Chem. C* **2015**, *3*, 8712.
[18] D. Pinkowicz, R. Podgajny, B. Nowicka, S. Chorazy, M. Reczyński, B. Sieklucka, *Inorg. Chem. Front.* **2015**, *2*, 10.
[19] J. M. Herrera, V. Marvaud, M. Verdaguer, J. Marrot, M. Kalisz, C. Mathonière, *Angew. Chem. Int. Ed.* **2004**, *43*, 5468; *Angew. Chem.* **2004**, *116*, 5584.
[20] N. Bridonneau, L. M. Chamoreau, G. Gontard, J. L. Cantin, J. von Bardeleben, V. Marvaud, *Dalton Trans.* **2016**, *45*, 9412.
[21] J. Long, L. M. Chamoreau, C. Mathonière, V. Marvaud, *Inorg. Chem.* **2009**, *48*, 22.
[22] R. Podgajny, T. Korzeniak, K. Stadnicka, Y. Dromzee, N. W. Alcock, W. Errington, K. Kruczala, M. Balanda, T. J. Kemp, M. Verdaguer, B. Sieklucka, *Dalton Trans.* **2003**, 3458.
[23] D. Brinzei, L. Catala, C. Mathonière, W. Wernsdorfer, A. Gloter, O. Stephan, T. Mallah, *J. Am. Chem. Soc.* **2007**, *129*, 3778.
[24] L. Catala, A. Gloter, O. Stephan, G. Rogez, T. Mallah, *Chem. Commun.* **2006**, 1018.
[25] N. Bridonneau, J. Long, J. L. Cantin, J. von Bardeleben, D. R. Talham, V. Marvaud, *RSC Adv.* **2015**, *5*, 16696.
[26] S. Tricard, F. Charra, T. Mallah, *Dalton Trans.* **2013**, *42*, 15835.
[27] F. Volatron, D. Heurtaux, L. Catala, C. Mathonière, A. Gloter, O. Stephan, D. Repetto, M. Clemente-Leon, E. Coronado, T. Mallah, *Chem. Commun.* **2011**, *47*, 1985.
[28] J. Long, L. M. Chamoreau, V. Marvaud, *Eur. J. Inorg. Chem.* **2011**, 4545.
[29] J. H. Lim, Y. S. You, H. S. Yoo, J. H. Yoon, J. I. Kim, E. K. Koh, C. S. Hong, *Inorg. Chem.* **2007**, *46*, 10578.
[30] L. Catala, T. Mallah, *Coord. Chem. Rev.* **2017**, *346*, 32.
[31] E. Chelebaeva, J. Larionova, Y. Guari, R. A. S. Ferreira, L. D. Carlos, A. A. Trifonov, T. Kalaivani, A. Lascialfari, C. Guerin, K. Molvinger, L. Datas, M. Maynadier, M. Gary-Bobo, M. Garcia, *Nanoscale* **2011**, *3*, 1200.
[32] M. A. Carvajal, R. Caballol, C. de Graaf, *Dalton Trans.* **2011**, *40*, 7295.
[33] N. Bridonneau, J. Long, J.-L. Cantin, J. von Bardeleben, S. Pillet, E. E. Bendeif, D. Aravena, E. Ruiz, V. Marvaud, *Chem. Commun.* **2015**, *51*, 8229.
[34] S.-i. Ohkoshi, H. Tokoro, *Acc. Chem. Res.* **2012**, *45*, 1749.
[35] D. Pinkowicz, B. Czarnecki, M. Reczynski, M. Arczynski, *Sci. Prog.* **2015**, *98*, 346.
[36] P. Chakraborty, C. Enachescu, C. Walder, R. Bronisz, A. Hauser, *Inorg. Chem.* **2012**, *51*, 9714.
[37] S. Schenker, A. Hauser, W. Wang, I. Y. Chan, *J. Chem. Phys.* **1998**, *109*, 9870.
[38] a) S. Pillet, E. E. Bendeif, S. Bonnet, H. J. Shepherd, P. Guionneau, *Phys. Rev. B* **2012**, *86*, 064106; b) E. Milin, V. Patinec, S. Triki, E. E. Bendeif, S. Pillet, M. Marchivie, G. Chastanet, K. Boukheddaden, *Inorg. Chem.* **2016**, *55*, 11652; c) V. Legrand, S. Pillet, C. Carbonera, M. Souhassou, J.-F. Létard, P. Guionneau, C. Lecomte, *Eur. J. Inorg. Chem.* **2007**, 5693.
[39] M. R. Pressprich, M. A. White, Y. Vekhter, P. Coppens, *J. Am. Chem. Soc.* **1994**, *116*, 5233.
[40] a) F. Matthieu, M. F. Dumont, O. N. Risset, E. S. Knowles, T. Yamamoto, D. M. Pajerowski, M. W. Meisel, D. R. Talham, *Inorg. Chem.* **2013**, *52*, 4494; b) E. Coronado, M. C. Gimenez-Lopez, G. Levchenko, F. M. Romero, V. Garcia-Baonza, A. Milner, M. Paz-Pasternak, *J. Am. Chem. Soc.* **2005**, *127*, 4580–4581.
[41] M. Koziel, R. Podgajny, R. Kania, R. Lebris, C. Mathonière, K. Lewinski, K. Kruczala, M. Rams, C. Labrugere, A. Bousseksou, B. Sieklucka, *Inorg. Chem.* **2010**, *49*, 2765.
[42] K. Malka, J. Aubard, M. Delamar, V. Vivier, M. Che, C. Louis, *J. Phys. Chem. B* **2003**, *107*, 10494.
[43] M. A. Arrio, J. Long, C. Cartier dit Moulin, A. Bachschmidt, V. Marvaud, A. Rogalev, C. Mathonière, F. Wilhelm, P. Sainctavit, *J. Phys. Chem. C* **2010**, *114*, 593.
[44] S.-i. Ohkoshi, H. Tokoro, T. Hozumi, Y. Zhang, K. Hashimoto, C. Mathonière, I. Bord, G. Rombaut, M. Verelst, C. Cartier dit Moulin, F. Villain, *J. Am. Chem. Soc.* **2006**, *128*, 270.
[45] B. Bechlars, D. M. d'Alessandro, D. M. Jenkins, A. T. Iavarone, S. D. Glover, C. P. Kubiak, J. R. Long, *Nat. Chem.* **2010**, *2*, 362.

[46] O. Kahn, *Molecular Magnetism*, VCH, Weinheim, **1993**.
[47] A. Rodríguez-Fortea, P. Alemany, S. Alvarez, E. Ruiz, A. Scuiller, C. Decroix, V. Marvaud, J. Vaissermann, M. Verdaguer, I. Rosenman, M. Julve, *Inorg. Chem.* **2001**, *40*, 5868.
[48] F. Tuyèras, A. Scuiller, C. Guyard-Duhayon, M. Hernandez-Molina, F. Fabrizi de Biani, M. Verdaguer, T. Mallah, W. Wernsdorfer, V. Marvaud, *Inorg. Chim. Acta* **2008**, *361*, 3505.

Received: August 15, 2017